AUTOMATED VARIANCE REDUCTION APPLIED TO NUCLEAR WELL-LOGGING PROBLEMS

RADIATION PROTECTION

KEYWORDS: *Monte Carlo, nuclear well-logging, variance reduction*

JOHN C. WAGNER,* DOUGLAS E. PEPLOW, and THOMAS M. EVANS
Oak Ridge National Laboratory, Nuclear Science and Technology Division, P.O. Box 2008, Oak Ridge, Tennessee 37831-6170

Received July 14, 2008
Accepted for Publication November 28, 2008

Simulating nuclear well-logging devices with Monte Carlo methods is computationally challenging and requires significant variance reduction to compute detector responses with low statistical uncertainties in reasonable lengths of time. The consistent adjoint-driven importance sampling (CADIS) method, which provides consistent source and transport biasing parameters based on a deterministic adjoint (importance) function, has been demonstrated to be very effective for well-logging simulations and other deep-penetration problems. A recent extension to the CADIS method, FW-CADIS (forward-weighted CADIS), is designed to optimize the calculation of several tallies at once by using an adjoint function based on an adjoint source weighted by the inverse of the forward flux. These advanced variance reduction methods have been incorporated and automated into the MAVRIC sequence of SCALE, making them very easy to use. The CADIS and FW-CADIS methods are demonstrated and compared on simple benchmark models of both neutron- and photon-based well-logging devices. Both advanced variance reduction methods offer a substantial reduction in computing time, compared to analog simulation, for these applications.

I. INTRODUCTION

The Monte Carlo method enables detailed, explicit geometric, energy, and angular representations and hence is considered to be the most accurate method available for solving complex radiation transport problems. Because of its associated accuracy, the Monte Carlo method is widely used in the petroleum exploration industry to design, benchmark, and simulate nuclear well-logging tools. Nuclear well-logging tools, which contain neutron and/or gamma sources and two or more detectors, are placed in boreholes that contain water (and possibly other fluids) and that are typically surrounded by a formation (e.g., limestone, sandstone, calcites, or a combination). The response of the detectors to radiation returning from the surrounding formation is used to infer information about the material porosity, density, composition, and associated characteristics. Accurate computer simulation is a key aspect of this exploratory technique. However, because this technique involves calculating highly precise responses (at two or more detectors) based on radiation that has interacted with the surrounding borehole and formation, the transport simulations are computationally intensive, requiring significant use of variance reduction techniques, parallel computing, or both.

Because of the challenging nature of these problems, nuclear well-logging problems have frequently been used to evaluate the effectiveness of variance reduction techniques.[1–4] The focus of these works has been on improving the computational efficiency associated with calculating the response at a given detector location. However, since the actual objective of nuclear well-logging tool simulations is to calculate the response at each of a series of detectors with some acceptably small statistical uncertainty, the approaches described in those works involve a separate calculation for each detector in the well-logging tool. In contrast, this work investigates the simultaneous optimization of multiple detectors (in a single calculation).

This paper summarizes recent work to apply, evaluate, and compare deterministic adjoint-based variance reduction methods, including a recently developed method for simultaneous optimization of multiple detectors, using two simple nuclear well-logging tool problems that have

*E-mail: wagnerjc@ornl.gov

been widely used in the variance reduction literature. The computational effectiveness of the method for simultaneous optimization is also compared to the use of multiple individually optimized simulations for these simple well-logging problems.

II. METHODS

Advanced automated variance reduction methods that use approximate forward and/or adjoint fluxes to generate consistent source and transport biasing parameters for accelerating Monte Carlo simulations have been developed and implemented at Oak Ridge National Laboratory for use with the standardized computer analyses for licensing evaluation (SCALE) and Monte Carlo N-particle (MCNP) codes.[5,6] For accelerating Monte Carlo calculations of localized quantities (e.g., a detector tally), the consistent adjoint-driven importance sampling (CADIS) method,[7] which uses an approximate adjoint solution to determine consistent source and transport (weight windows) biasing parameters, is used.

Alternatively, for accelerating Monte Carlo calculations of either mesh tallies or multiple localized quantities (e.g., multiple detector tallies), the forward-weighted CADIS (FW-CADIS) method[8] may be used. FW-CADIS uses an approximate forward solution to weight the source in an adjoint calculation such that the resulting adjoint importance function represents the importance of particles to achieving uniformly distributed Monte Carlo particles throughout the requested tally regions. The premise for the FW-CADIS method is that uniformly distributed Monte Carlo particles should roughly correspond to uniform statistical uncertainties in those regions. As implemented, the approximate forward and/or adjoint fluxes are generated by deterministic transport calculations from either the Denovo or TORT three-dimensional discrete ordinates codes. Because these methods involve the combined use of deterministic and Monte Carlo transport methods, they are referred to as hybrid methods. The CADIS and FW-CADIS methods have been fully implemented and automated in the Monaco with automated variance reduction using importance calculations (MAVRIC) sequence[9] being developed for public release in SCALE 6. The calculations performed for this paper were all done with MAVRIC. More details about CADIS, FW-CADIS, MAVRIC, Denovo, and Monaco are given in a companion article[10] also appearing in this special issue.

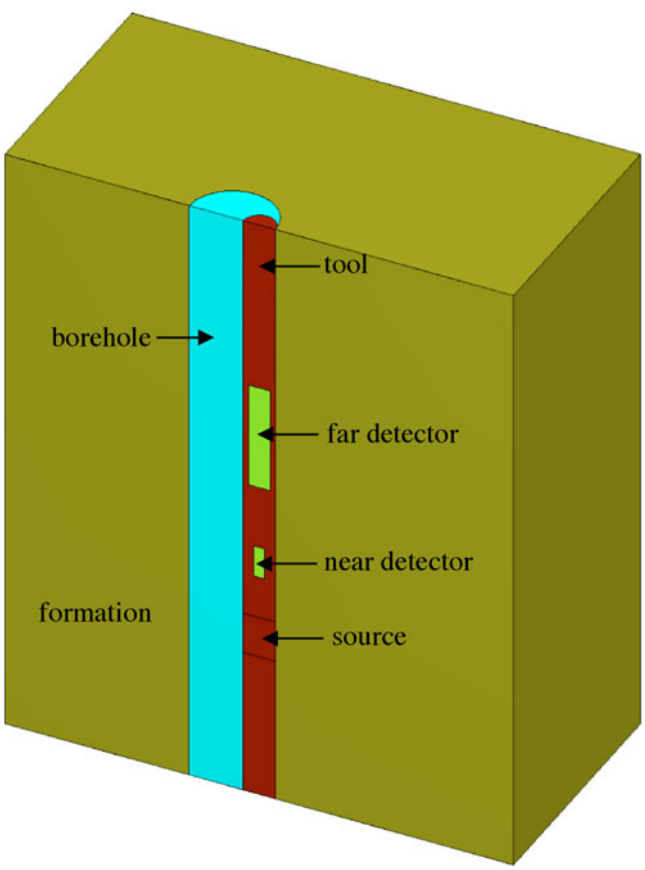

Fig. 1. Monte Carlo model of the neutron porosity tool.

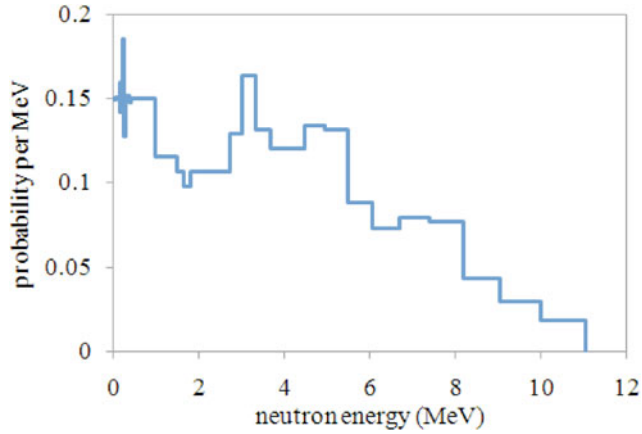

Fig. 2. Neutron source energy distribution.

III. CALCULATIONS

Three methods were applied to representative models of a neutron porosity tool and a gamma-ray lithodensity tool, each containing two detectors (one near and one far). First, a reference, essentially analog,[a] Monte

[a]Note that the default in Monaco is to use implicit capture and Russian roulette with a lower weight limit. Hence, although the baseline simulation is not truly analog, for simplicity in referencing it is referred to throughout this paper as analog.

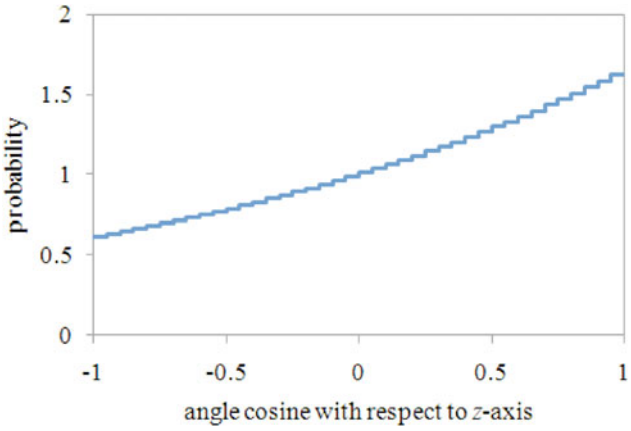

Fig. 3. Neutron source direction distribution.

Carlo calculation was performed to serve as a baseline. Second, a pair of calculations were performed using the standard CADIS method to demonstrate its effectiveness for optimizing the computation of each detector response separately. Finally, the newly developed FW-CADIS method was applied to demonstrate and evaluate its effectiveness for simultaneous optimization of both detectors in a single simulation. All calculations for this paper were performed on a single Linux-based 64-bit processor.

Previous work[4] has demonstrated the greater efficiencies of the CADIS methodology compared to manual optimization and use of the MCNP weight window generator for individual detector responses in nuclear well-logging applications. Thus, such comparisons were not made in this work.

III.A. Neutron Porosity Tool

The neutron porosity tool model used in this study is MCNP sample problem 12, which was converted into a MAVRIC model. The geometric description for MAVRIC is reduced to just the physical geometry, shown in Fig. 1, without the extraneous geometric cells and surfaces required by the MCNP cell-based weight windows. The 7.62-cm-diam iron tool is located against the wall of the 20.32-cm-diam borehole filled with water. The near detector is a 2.54-cm-diam, 7.62-cm-high cylinder whose center is located 19 cm above the center of the source region. The far detector is much larger, with a diameter of 5.08 cm and a length of 25.4 cm. Its center is located 50.8 cm from the source. The source region is a 7.6-cm-diam, 10-cm-long cylinder located at the origin. The extent of the modeled limestone formation is 120 × 120 × 145 cm. The formation porosity is 20 porosity units (p.u.).[b]

[b] A unit equal to the percentage of pore space in a unit volume of rock that lies between 0 and 100.

As in the original MCNP sample problem, the neutron source has a strength of 7.4×10^{11} n/s, with an energy spectra as shown in Fig. 2. The directional distribution is preferentially upward, toward the detectors,

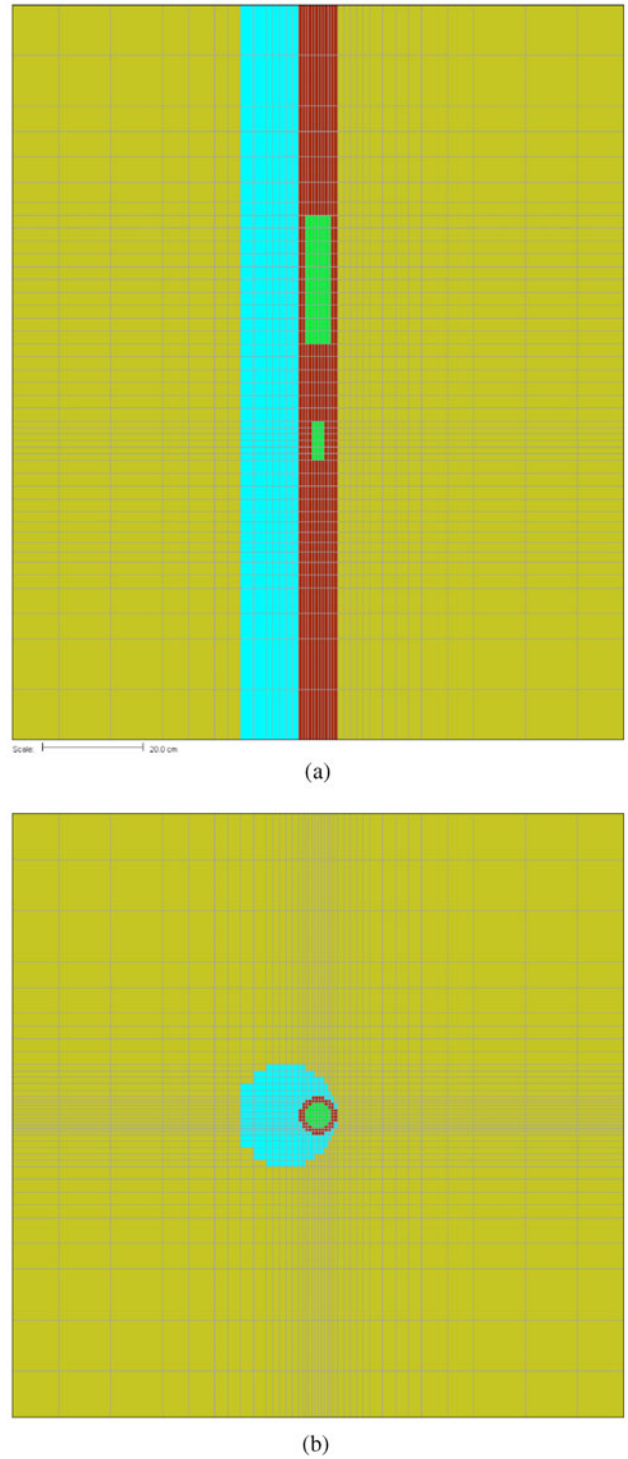

Fig. 4. Discrete ordinates model of the neutron porosity tool with (a) an *x*-*z* view and (b) an *x*-*y* view.

as shown in Fig. 3. The detector response is the neutron flux convoluted with the $^3He(n,p)^3H$ cross section, integrated over the volume of each detector, yielding a final response with units of charged pairs per second.

MAVRIC and its underlying Monte Carlo transport code, Monaco, are multigroup codes. For this problem, the BUGLE-96 broad-group library[11] (without upscattering) was used for both the Denovo discrete ordinates and Monaco Monte Carlo calculations. Since the multigroup library used has only five groups below 5 eV and did not include upscattering, future work is planned to evaluate the impact of using a multigroup library with more thermal groups and upscattering.

The Denovo discrete ordinates calculations used an S_8 quadrature and a P_3 Legendre expansion order for the scattering cross sections. A fairly fine mesh was used, with $40 \times 40 \times 44 = 70\,400$ cells, as shown in Fig. 4.

III.B. Gamma-Ray Litho-Density Tool

The gamma-ray litho-density tool is taken from the benchmark described by Gardner and Verghese[12] and is shown in Fig. 5. This model uses a 10-cm-diam tool made of iron (with a tungsten density) in a 20-cm borehole filled with water. The near detector is a 2-cm-diam, 2-cm-long cylinder located 20 cm from the source.

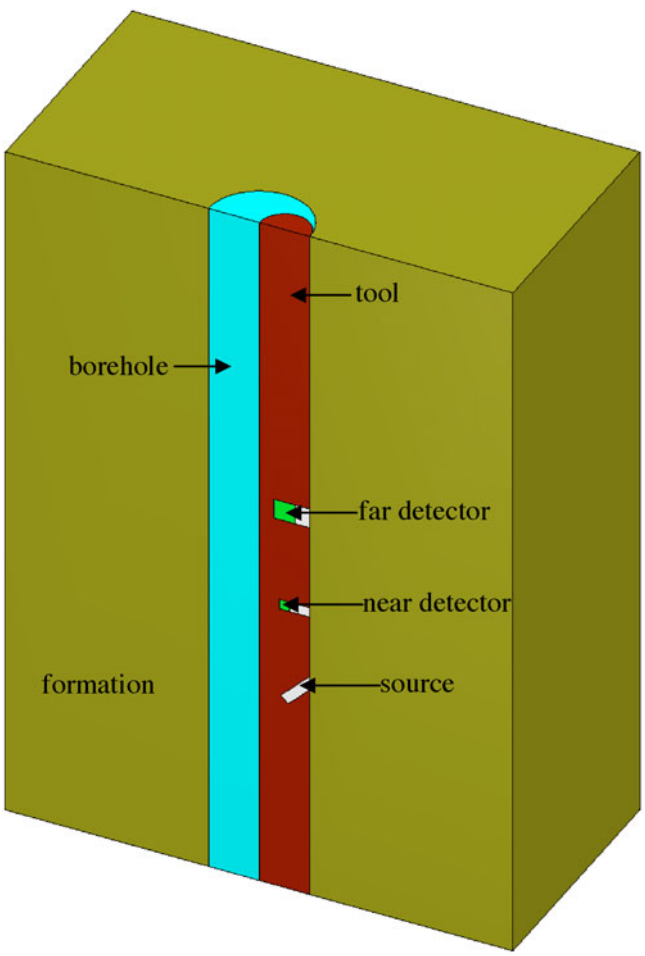

Fig. 5. Monte Carlo model of the gamma-ray litho-density tool.

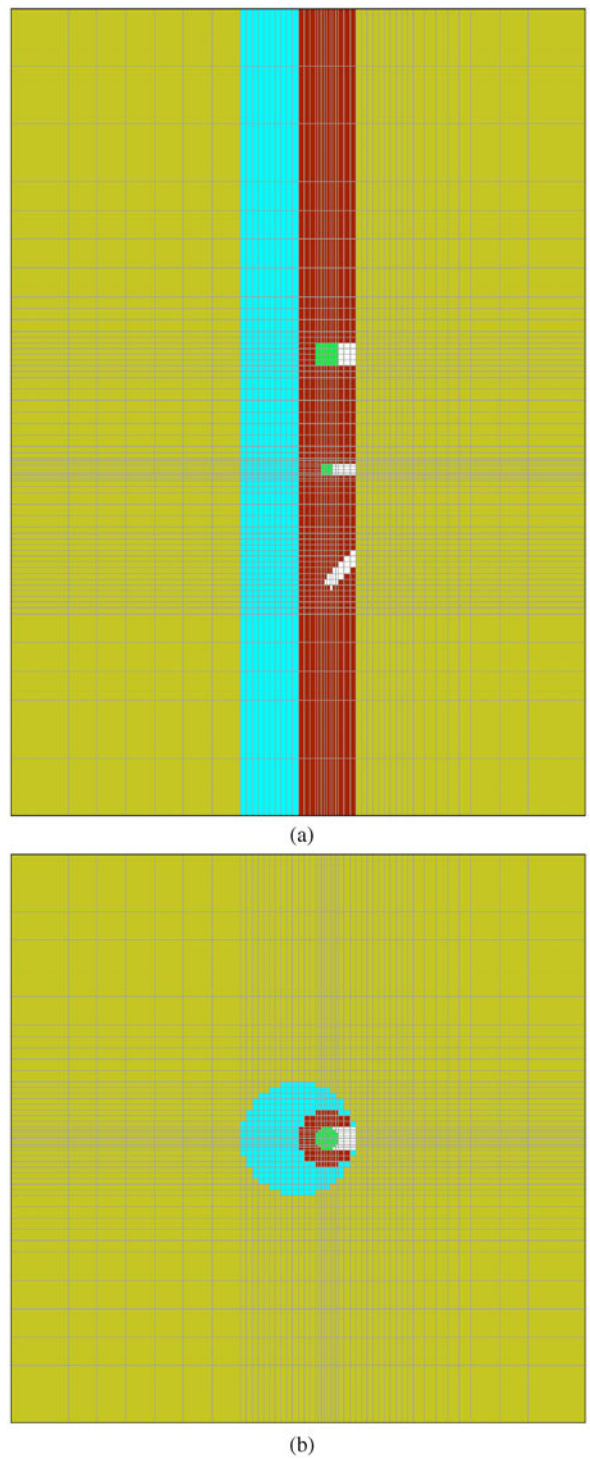

Fig. 6. Discrete ordinates model of the gamma-ray litho-density tool with (a) an x-z view and (b) an x-y view.

The far detector is a 4- × 4-cm cylinder located 40 cm from the source. Each detector is made of NaI and collimated to look out into the formation. The source is contained in an angled collimater, aiming upward and into the formation. The collimators are filled with oxygen. The extent of the modeled formation is 100 × 100 × 140 cm.

The source is an isotropic ^{137}Cs source with a strength of 10^{11} photons/s (661.7 keV). The new SCALE multigroup (27-neutron/19-photon) library based on ENDF/B-VII.0 data[13] was used for both the discrete ordinates and Monte Carlo calculations. For the MAVRIC calculations, the source is represented by one photon group from 600 to 800 keV, and the source strength was modified so that the total energy emitted was preserved. For these calculations, no response function is used—the goal of this example is to calculate total photon flux within each detector volume.

The Denovo calculations used S_8 quadrature and P_3 Legendre order. The mesh grid used 49 × 43 × 59 = 124 313 cells, with particular emphasis on geometric representation of the collimators to ensure accurate importance maps. This is shown in Fig. 6.

IV. RESULTS

IV.A. Neutron Porosity Tool

The results from applying the three different methods to the neutron porosity tool (using four simulations) are summarized in Table I. In addition to calculation of the detector responses for each simulation, MAVRIC also computed a mesh tally along the $y = 0$ plane to show where the neutrons were being followed. Figure 7 shows that the analog simulation tracks particles deep into the rock formation, where they have little chance of contributing to either detector. Not shown in the figure is the energy dependence—the analog simulation spends excess time tracking thermal neutrons throughout the geometry when only the neutrons that thermalize close to the detector contribute to the detector response. This is why the near detector tally converges so slowly and the far detector even more slowly. After 15 h of computation time, the relative uncertainty for the near detector is <1% and that for the far detector is 2%.

Using the CADIS method to optimize the Monte Carlo calculation for each detector separately, speedups

TABLE I

Results for the Neutron Porosity Tool

	Analog	CADIS		FW-CADIS
		Near[a]	Far[b]	
Simulation times (min)				
Forward discrete ordinates	—	—	—	8
Adjoint discrete ordinates	—	9	9	9
Monte Carlo	904	125	123	122
Near detector				
Charged pairs/s	8.820E+08[c]	8.814E+08	7.805E+08	8.837E+08
Relative uncertainty	0.78%	0.17%	7.16%	0.18%
Far detector				
Charged pairs/s	1.793E+08	1.155E+08	1.832E+08	1.833E+08
Relative uncertainty	2.13%	54.17%	0.27%	0.65%
Monte Carlo FOM ratio[d]				
Near detector	1	154	—	132
Far detector	1	—	457	78
Time (min) required to achieve 1% relative uncertainty				
Near detector	545	13	—	21
Far detector	4088	—	18	69
Time (min) required				
For both detectors	4088	31		69
Time improvement				
Speedup over analog	1	132		59

[a]CADIS method optimized for the near detector.
[b]CADIS method optimized for the far detector.
[c]Read as 8.820×10^8.
[d]FOM = figure of merit = $1/[(\mathrm{RE})^2 T]$, where RE is the relative error and T is computer time.

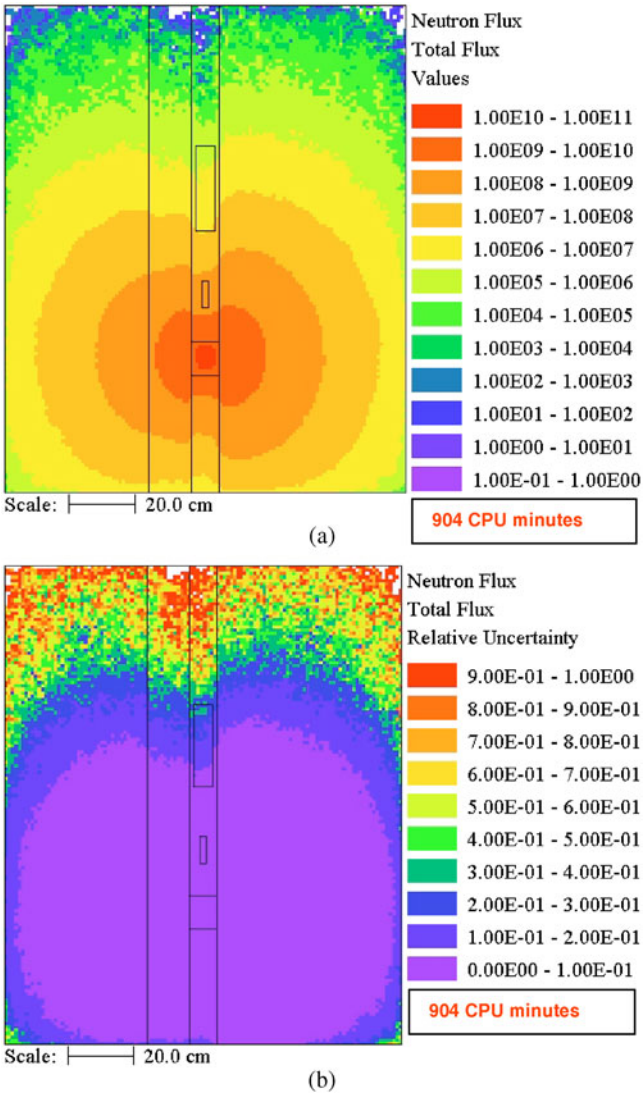

Fig. 7. (a) Total neutron flux and (b) its relative uncertainty for the neutron porosity tool from the analog calculation.

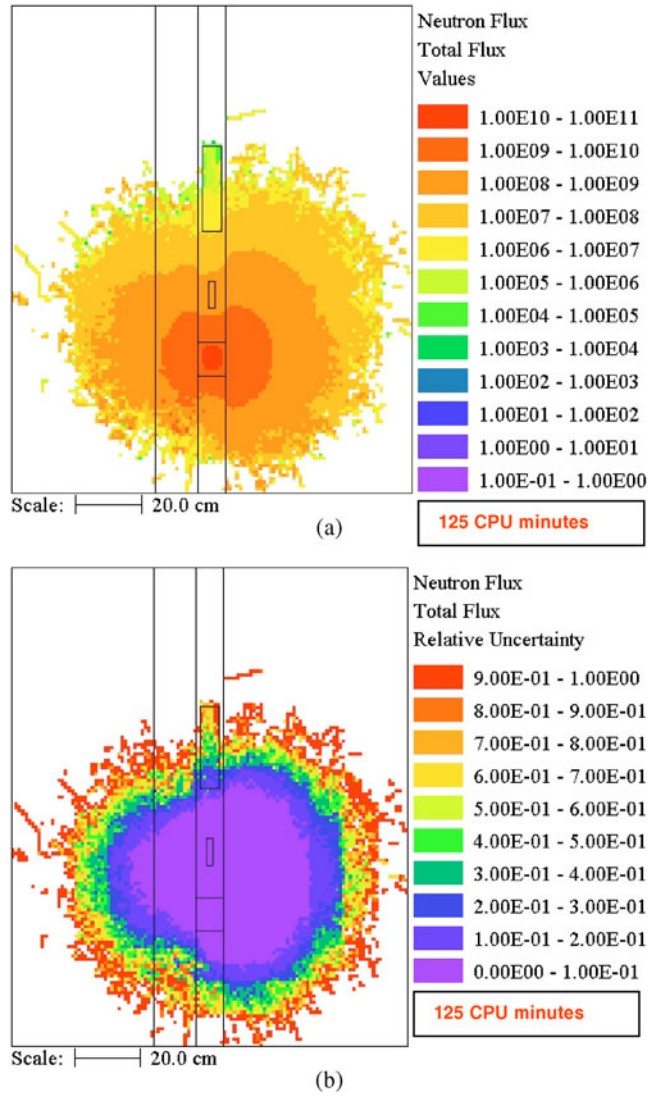

Fig. 8. (a) Total neutron flux and (b) its relative uncertainty for the neutron porosity tool from the CADIS calculation optimized for the near detector.

of 154 and 457 for the near and far detectors, compared to the analog simulation, were obtained. Typical to the method, more difficult problems benefit more from the combined importance map/biased source than easier problems. The source and transport biasing require the Monte Carlo simulation to spend more time on the particles in spatial and energy domains that contribute the most to the desired response. For the CADIS simulation optimized for the near detector, Fig. 8 shows that particles are not tracked to the far reaches of the formation; instead, time is spent on the particles near the detector (and on the particles with energies that contribute to the response). The CADIS simulation optimized for the far detector, in Fig. 9, shows similar effects. Note that optimization for one detector comes at the expense of greater uncertainty for the other. For example, when the adjoint source is located at the far detector, one might initially expect that the near detector efficiency would also improve. However, this is not the case—the relative uncertainty for the near detector is 25 times larger than for the far detector. This result is appropriate and consistent with the optimization goal.

The FW-CADIS method optimizes the calculation for the simultaneous evaluation of both detectors. As shown in Table I and Fig. 10, this method is effective at getting the particles to both detectors. Speedups compared to the analog calculation are 132 and 78 for the near and far detectors. It was anticipated that the FW-CADIS method (two discrete ordinates and one Monte Carlo) would perform as well as the separate CADIS

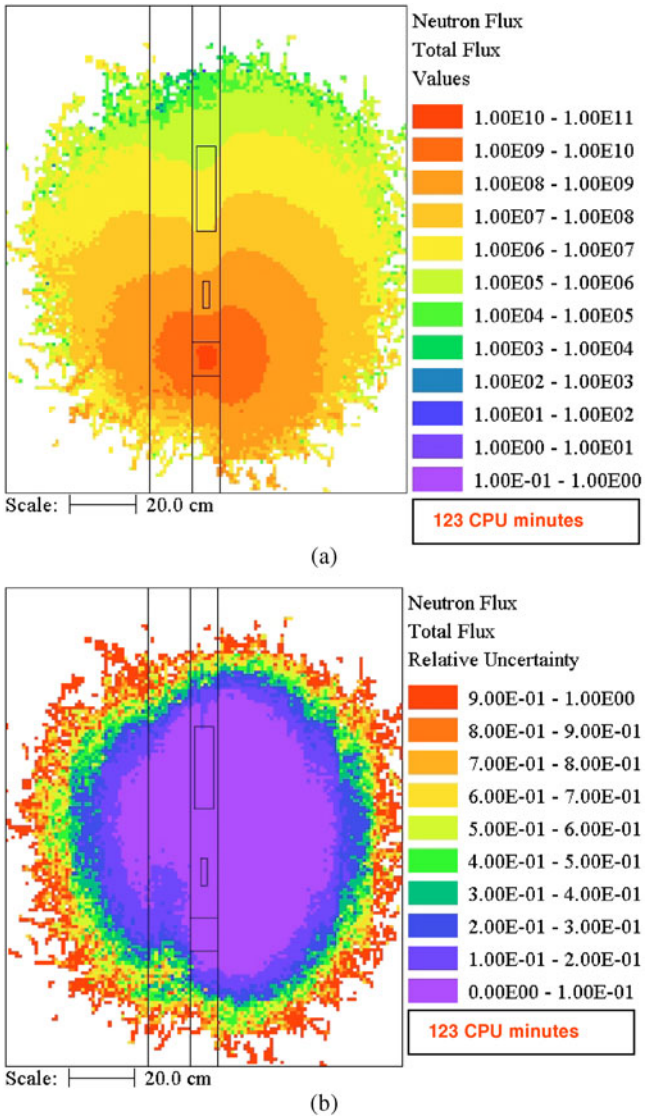

Fig. 9. (a) Total neutron flux and (b) its relative uncertainty for the neutron porosity tool from the CADIS calculation optimized for the far detector.

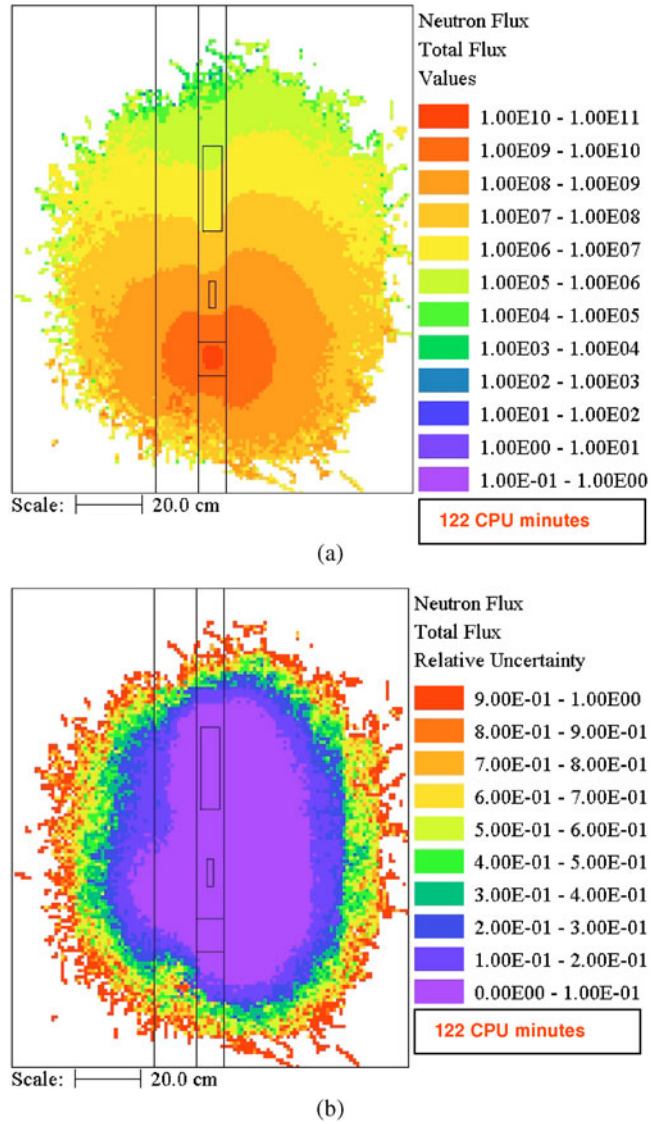

Fig. 10. (a) Total neutron flux and (b) its relative uncertainty for the neutron porosity tool from the FW-CADIS calculation.

calculations (two sets of calculations with one discrete ordinate and one Monte Carlo) for this problem with two detectors. The results presented in Table I show that for this neutron problem, the separate CADIS methods perform better. This may be due to the way the FW-CADIS method is implemented in MAVRIC: It is implemented to equalize the relative uncertainties in each mesh cell of each detector as opposed to equalizing the relative uncertainties in each of the detector regions as whole bodies. This implementation encourages more particles toward the far end of the far detector than are needed. Future work is planned to investigate this aspect of the implementation.

IV.B. Gamma-Ray Litho-Density Tool

The gamma-ray problem is a much more computationally challenging problem than the neutron tool problem; hence, more significant improvements are expected from the advanced variance reduction techniques. The results, summarized in Table II, show how difficult this problem is; after 46 h of computation the relative uncertainties for the near and far detectors are still 8 and 19%. Figure 11 shows the mesh tally and its relative uncertainty for the total photon flux in the analog calculation. Note that one portion of the far detector did not see any photons. Based on the 46-h run, it can be estimated that

TABLE II

Results for the Gamma-Ray Litho-Density Tool

	Analog	CADIS		FW-CADIS
		Near[a]	Far[b]	
Simulation times (min)				
Forward discrete ordinates	—	—	—	6
Adjoint discrete ordinates	—	7	7	7
Monte Carlo	2 762	126	123	126
Near detector				
Charged pairs/s	1.494E+03[c]	1.545E+03	0.000E+00	1.543E+03
Relative uncertainty	8.15%	0.46%	0.00%	0.61%
Far detector				
Charged pairs/s	6.130E+01	3.100E+03	5.587E+01	5.564E+01
Relative uncertainty	19.14%	65.24%	0.34%	0.43%
Monte Carlo FOM[d] ratio				
Near detector	1	6 830	—	3 867
Far detector	1	—	71 821	43 278
Time (min) required to achieve 1% relative uncertainty				
Near detector	183 547	34	—	60
Far detector	1 012 136	—	21	36
Time (min) required				
For both detectors	1 012 136	55		60
Time improvement				
Speedup over analog	1	18 402		16 869

[a]CADIS method optimized for the near detector.
[b]CADIS method optimized for the far detector.
[c]Read as 1.494×10^3.
[d]FOM = figure of merit = $1/[(\mathrm{RE})^2 T]$, where RE is the relative error and T is computer time.

to reach 1% relative uncertainty, the analog method would require just under 2 yr of computer time.

For the CADIS calculations, the speedups compared to analog were 6 830 and 71 821 for the near and far detectors, respectively, enabling results with 1% statistical uncertainties to be achieved in <1 h. Mesh tallies for these simulations are shown in Fig. 12 for the near detector and Fig. 13 for the far detector. Comparison of Figs. 12 and 13 to Fig. 11 clearly illustrates that with the CADIS calculations, computational effort is focused on the particles that contribute to the detector region being optimized. Like the neutron tools, when the simulation is optimized for one detector, the result for the other detector is not reliable.

The FW-CADIS performed just as well as the two separate CADIS calculations, calculating total photon flux in each detector with roughly the same relative uncertainty. Here, both results were obtained in one simulation in 1 h. Mesh tallies for this method are shown in Fig. 14. It is expected that for modern well-logging tools with considerably more than two detectors in one tool, the FW-CADIS method will prove to be more efficient than separate CADIS calculations. Using just one simulation for all the detectors has other practical benefits (e.g., easier to manage models and files).

V. CONCLUSIONS

The CADIS and FW-CADIS methods are both very effective for improving the computational efficiency of nuclear well-logging simulations. Typical to the methods, more difficult computational problems benefit more from the methods than easier problems; e.g., speedups for the gamma-ray tool were between 16 869 and 18 402, as compared to 59 to 132 for the neutron tool. Comparisons of individual detector optimizations via the CADIS method, which requires separate deterministic and Monte Carlo calculations for each detector, with simultaneous optimization via the FW-CADIS method, which requires two deterministic calculations and a single Monte Carlo calculation, indicate that both approaches yield similar overall computational efficiency. Because both methods are automated within MAVRIC, the user requirements associated with the application of either

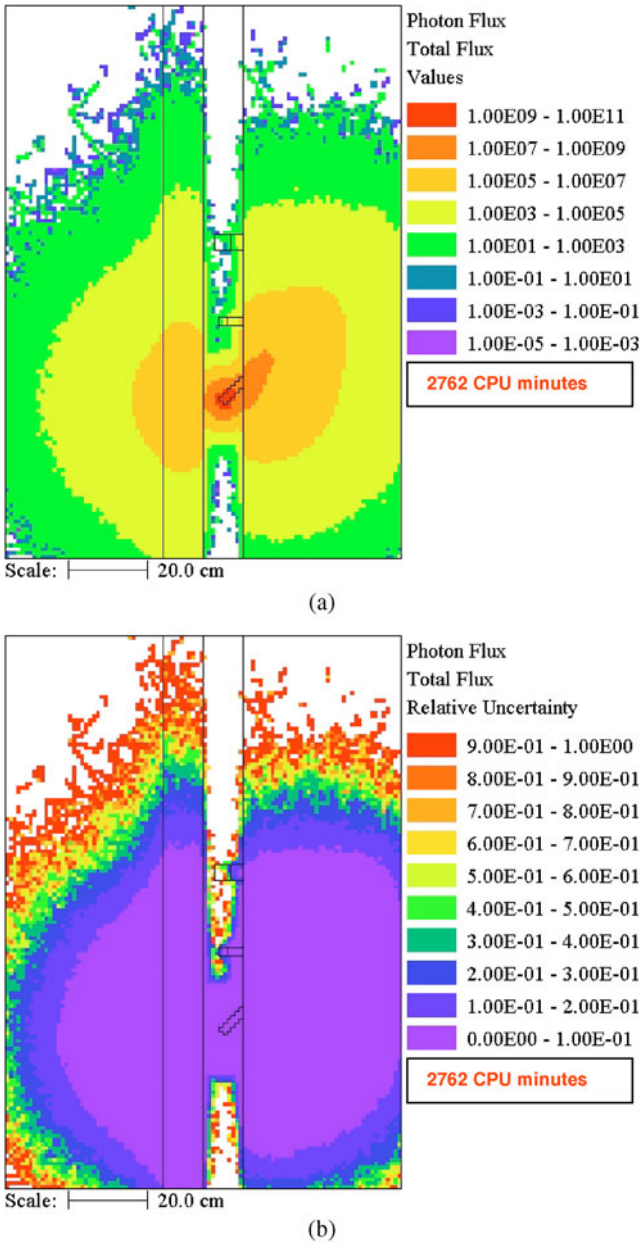

Fig. 11. (a) Total photon flux and (b) its relative uncertainty for the gamma-ray litho-density tool from the analog calculation.

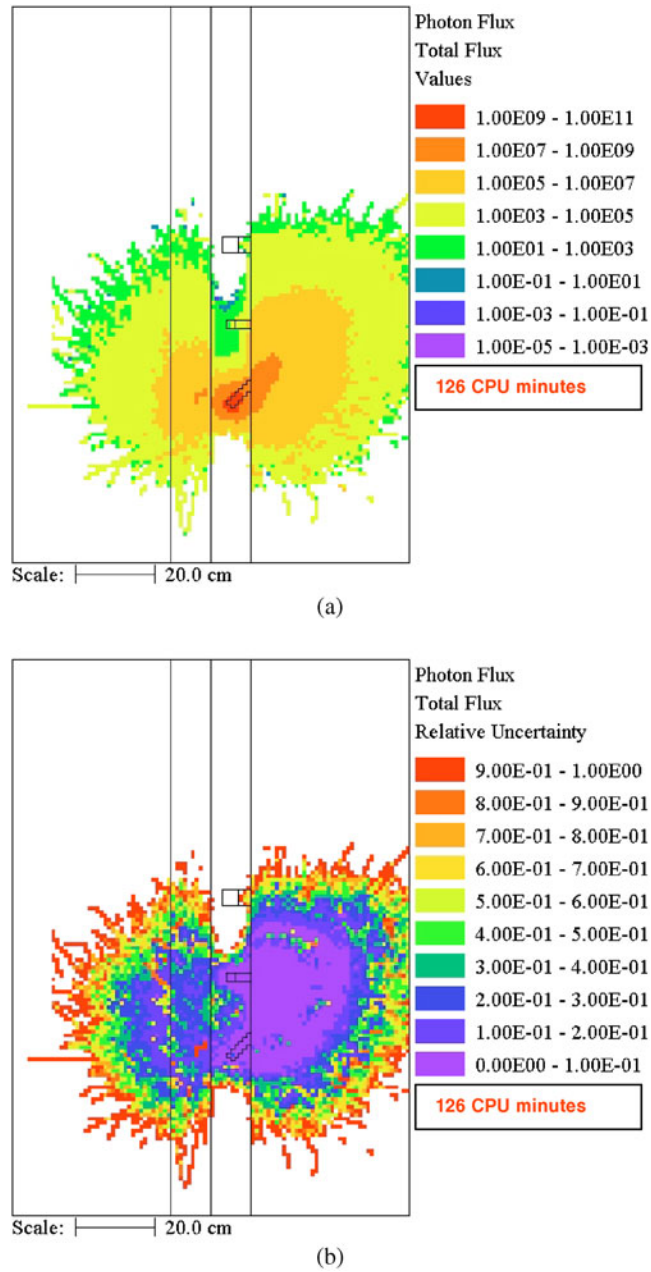

Fig. 12. (a) Total photon flux and (b) its relative uncertainty for the gamma-ray litho-density tool from the CADIS calculation optimized for the near detector.

method are minimal. Further, when using MAVRIC, only a single keyword change is required to select between the CADIS and FW-CADIS methods. However, because the FW-CADIS method simultaneously optimizes both detectors in a single MAVRIC calculation, whereas individual optimization of detectors with CADIS requires a separate MAVRIC calculation for each detector, application of the FW-CADIS approach is easier and more straightforward for the user. Although individual optimizations with CADIS outperformed the simultaneous optimization with FW-CADIS for the neutron problem in terms of total computational time required, the relative efficiency of the FW-CADIS approach is expected to increase as the number of detectors increases, because it does not require a separate calculation for each detector. Future work is planned to evaluate

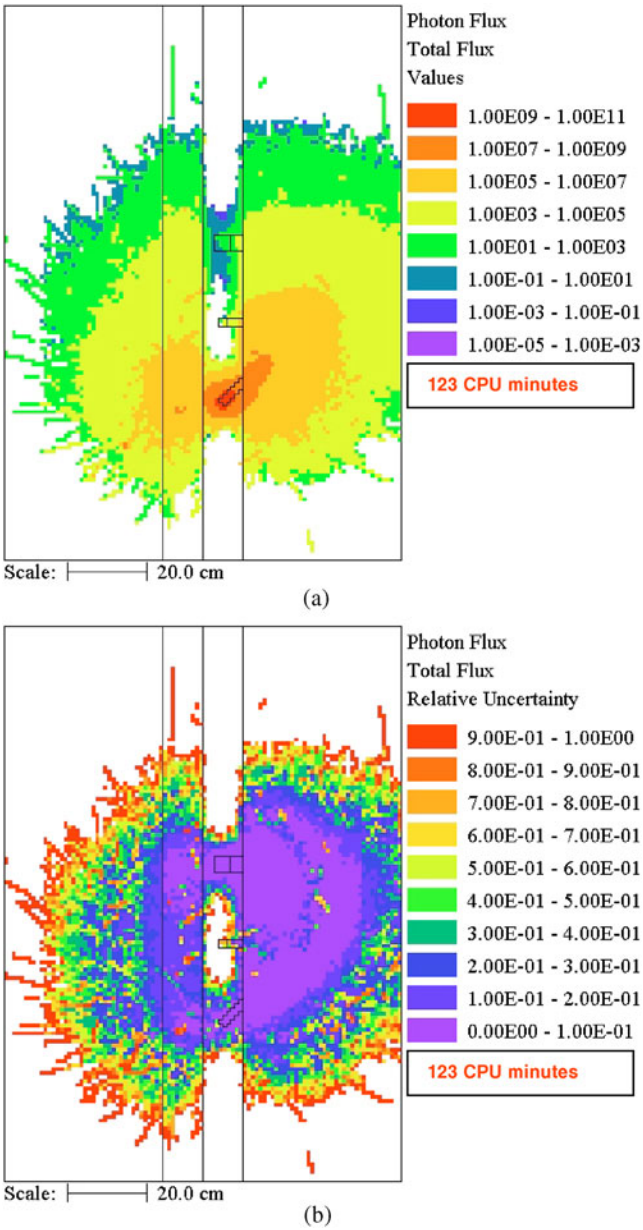

Fig. 13. (a) Total photon flux and (b) its relative uncertainty for the gamma-ray litho-density tool from the CADIS calculation optimized for the far detector.

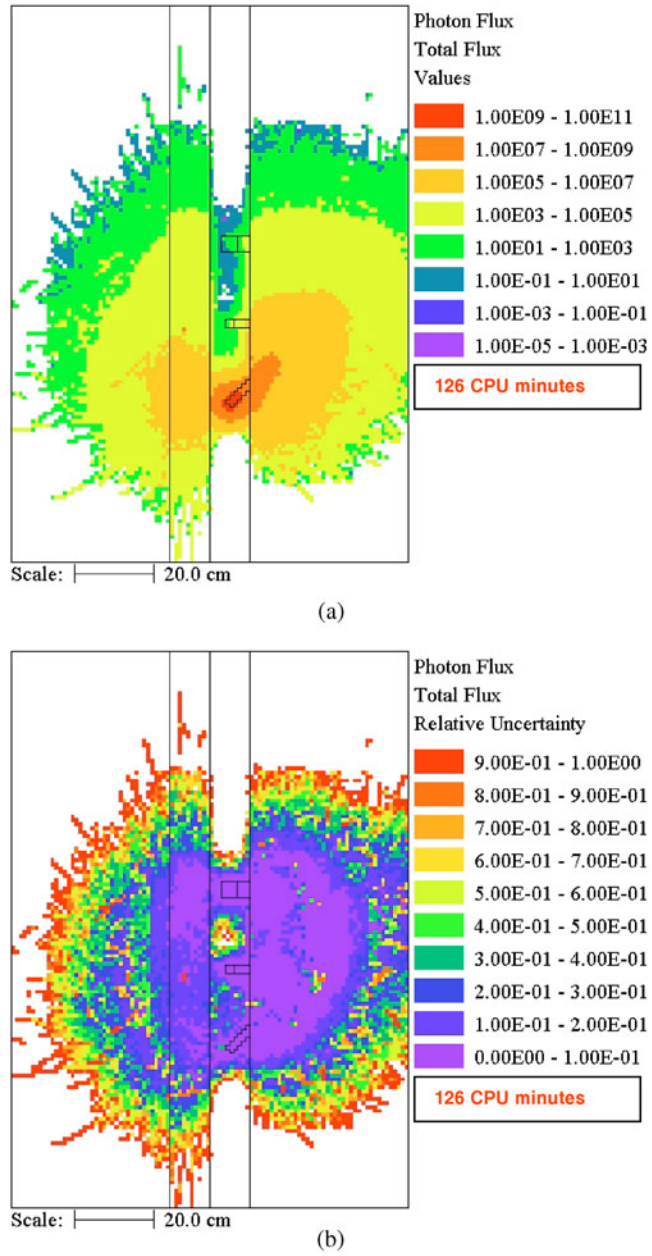

Fig. 14. (a) Total photon flux and (b) its relative uncertainty for the gamma-ray litho-density tool from the FW-CADIS calculation.

this expectation for nuclear well-logging tools that have three or more detectors and other relevant problems that involve multiple detectors.

ACKNOWLEDGMENTS

Work for this paper was supported by Oak Ridge National Laboratory, which is managed and operated by UT-Battelle, LLC, for the U.S. Department of Energy under contract DE-AC05-00OR22725.

REFERENCES

1. T. M. EVANS and T. A. WAREING, "The Solution of Well-Logging Problems Using Hybrid Transport Methods on Unstructured Meshes," *Proc. Conf. Mathematics and Computation, Reactor Physics and Environmental Analysis in Nuclear Applications*, Madrid, Spain, September 27–30, 1999, Vol. 2, p. 1393, Senda Editorial, S.A. (1999).

2. R. P. GARDNER and L. LIU, "Monte Carlo Simulation of Neutron Porosity Oil Well Logging Tools: Combining the

Geometry-Independent Fine-Mesh Importance Map and One-Dimensional Diffusion Model Approaches," *Nucl. Sci. Eng.*, **133**, 80 (1999).

3. K. A. VAN RIPER, T. J. URBATSCH, P. D. SORAN, D. K. PARSONS, J. E. MOREL, G. W. McKINNEY, S. R. LEE, L. A. CROTZER, F. W. BRINKLEY, J. W. ANDERSON, and R. E. ALCOUFFE, "AVATAR—Automatic Variance Reduction in Monte Carlo Calculations," *Proc. Joint Int. Conf. Mathematical Methods and Supercomputing in Nuclear Applications*, Saratoga Springs, New York, October 6–10, 1997, Vol. 1, p. 661, American Nuclear Society (1997).

4. J. C. WAGNER, "An Automated Deterministic Variance Reduction Generator for Monte Carlo Shielding Applications," *Proc. Am. Nucl. Soc. 12th Biennial Radiation Protection and Shielding Division Topical Meeting*, Santa Fe, New Mexico, April 14–18, 2002, American Nuclear Society (2002).

5. "SCALE: A Modular Code System for Performing Standardized Computer Analyses for Licensing Evaluation," Version 5, Vols. I–III, ORNL/TM-2005/39, available from Radiation Safety Information Computational Center at Oak Ridge National Laboratory as CCC-725 (Apr. 2005).

6. X-5 MONTE CARLO TEAM, "MCNP—A General Monte Carlo N-Particle Transport Code, Version 5, Vol. I: Overview and Theory," LA-UR-03-1987, Los Alamos National Laboratory, Los Alamos, New Mexico (2003).

7. J. C. WAGNER and A. HAGHIGHAT, "Automated Variance Reduction of Monte Carlo Shielding Calculations Using the Discrete Ordinates Adjoint Function," *Nucl. Sci. Eng.*, **128**, 186 (1998).

8. J. C. WAGNER, E. D. BLAKEMAN, and D. E. PEPLOW, "Forward-Weighted CADIS Method for Global Variance Reduction," *Trans. Am. Nucl. Soc.*, **97**, 630 (2007).

9. D. E. PEPLOW, S. M. BOWMAN, J. E. HORWEDEL, and J. C. WAGNER, "Monaco/MAVRIC: Computational Resources for Radiation Protection and Shielding in SCALE," *Trans. Am. Nucl. Soc.*, **95**, 669 (2006).

10. D. E. PEPLOW, T. M. EVANS, and J. C. WAGNER, "Simultaneous Optimization of Tallies in Difficult Shielding Problems," *Nucl. Technol.*, **168**, 785 (2009).

11. J. E. WHITE, D. T. INGERSOLL, R. Q. WRIGHT, H. T. HUNTER, C. O. SLATER, N. M. GREENE, R. E. MacFARLANE, and R. W. ROUSSIN, "Production and Testing of the Revised VITAMIN-B6 Fine-Group and the BUGLE-96 Broad-Group Neutron/Photon Cross-Section Libraries Derived from ENDF/B-VI.3 Nuclear Data," NUREG/CR-6214, Rev. 1 (ORNL/TM-6795/R1), prepared for the U.S. Nuclear Regulatory Commission by Oak Ridge National Laboratory (Apr. 2000).

12. R. P. GARDNER and K. VERGHESE, "Monte Carlo Nuclear Well Logging Benchmark Problems with Preliminary Intercomparison Results," *Nucl. Geophys.*, **5**, *4*, 429 (1991).

13. D. WIARDA, M. E. DUNN, D. E. PEPLOW, T. M. MILLER, and H. AKKURT, "Development and Testing of ENDF/B-VI.8 and ENDF/B-VII.0 Coupled Neutron-Gamma Libraries for SCALE 6," NUREG/CR-6990, ORNL/TM-2008/047, U.S. Nuclear Regulatory Commission (Feb. 2009).